# Large Eddy Simulation of Fluid–Structure Interaction for Two Elastic Cylinders in Axial Flow


**Yu Cao, Kangfei Shi, and Zhanying Zheng**

**Abstract** The axial-flow-induced vibration (AFIV) of fuel rods in the nuclear power plant is closely related to nuclear safety. In this article, a numerical study of two elastic cylinders arranged side by side in axial flow is performed using the two-way fluid–structure coupling simulation. Large eddy simulation (LES) is employed to predict the turbulent flow. The root-mean-square (rms) vibration amplitude of the cylinder and the critical velocity of buckling instability are found to be in good agreement with experimental data. The vibration of two cylinders in axial flow are simulated at different dimensionless velocities $u^*$ ranging from 1.20 to 6.20, turbulence intensity $T_u$ and space ratio $P/D$. Results show that at low $T_u$ (0.7%), when $u^*$ reaches 4.56, both cylinders start to bend outward while vibrating. At higher $T_u$ (2.9 and 5.0%), the two cylinders recover from the outward bending positions. Although $T_u$ significantly affects the amplitude of cylinders, it does not change the vibration frequency of the cylinder and the critical velocity at which buckling instability occurs. As the gap is sufficiently small, the vibration amplitude does not show considerable variation laterally but enhances significantly along the centreline direction.

**Keywords** Dual elastic cylinder · Fluid–structure interaction · Axial-flow-induced vibration

## 1 Introduction

Axial-flow-induced vibration (AFIV) of slender fuel rods is an important safety concern in nuclear reactors.

Early efforts have been focused on the developing of linear and non-linear theories to predict the occurrences of instabilities. Païdoussis [1] reviewed early studies and summarized four classes of problems with the discussions focused on the stability characteristics. Wang et al. [2] later made a critical review on the vibrations and stability of a single or a cluster of cylinders subjected to axial flow or quiescent fluid,

Y. Cao · K. Shi · Z. Zheng (✉)
Center for Turbulence Control, Harbin Institute of Technology, Shenzhen, China
e-mail: zhengzhanying@hit.edu.cn



D. Kim et al. (eds.), *Fluid-Structure-Sound Interactions and Control*, Lecture Notes in Mechanical Engineering, https://doi.org/10.1007/978-981-97-6211-8_21

indicating that rich dynamical behaviours were evident. Although some theoretical models have achieved successes, the effects of turbulence accurately are unable to describe. But, it's crucial to both the quantification of subcritical vibration amplitude and onset of instabilities. Numerical simulations coupling fluid and structure solvers show some great advantages in this case, including the elimination of empirical relations, as well as the free of limitations on flow conditions and structure configurations. Numerical simulations of AFIV only started to appear since last decade, and the turbulent fluid field was also described using URANS (unsteady Reynolds-averaged Navier–Stokes) equations in some studies. De Ridder et al. [3] studied that both vibrations of a brass cylinder in axial water flow and the predicted frequencies of modes, which has a good agreement with linear theory in genera. Several attempts were made to adopt large eddy simulation (LES) for the prediction of fluid flow to overcome the limitations of URANS on the capture of small-scale turbulent structures, including the turbulent-induced vibration in an axial annual flow [4] and AFIV of a wire-wrapped tube bundle [5]. Recently, Lu et al. [6] carried out LES to study the AFIV of an isolated elastic cylinder, and largely resolved various turbulent structures around the cylinder, resulting in an in-depth understanding of the effect of incident turbulence intensity. In this study, the above approach is extended to the discussion of AFIV of two parallel elastic cylinders, with the emphasis on identifying the coupling effect between the cylinders and their influence on AFIV characteristics.

## 2 Methodologies

The two elastic cylinders are placed parallelly and surrounded by axial flow along the $z$ direction, as illustrated in Fig. 1, where $D$ is the cylinder diameter and $P$ is the centre-to-centre distance between the cylinders. Both cylinder ends are clamped, and the computational domain has a cylindrical shape. The flow enters the domain from the inlet with a uniform velocity $U_\infty$ and turbulent intensity $T_u$. The arbitrary Lagrangian–Eulerian (ALE) method is adopted to solve the governing equations. LES is employed to predict the turbulent flow, and a two-way fluid–structure coupling is achieved via an iterative process between fluid and structure solvers. At each time step ($\Delta t = 0.005$ s), the two solvers exchange fluid force and vibration displacement based on a Gauss–Seidel iteration, until convergence is obtained. Moreover, the related dimensionless parameters are defined as follows:

$$\begin{aligned} &C_p = (p - p_\infty)/\left(1/2\rho U_\infty^2\right),\ u^* = U_\infty L(\rho A_c/EI)^{1/2}, \\ &t^* = \left(t/L^2\right)[EI/(\rho + \rho_c)A_c]^{1/2},\ A_x^* = a_x/D, \\ &A_y^* = a_y/D,\ A_{xrms}^* = A_{xrms}/D,\ A_{yrms}^* = A_{yrms}/D, \\ &f^* = fL^2[(\rho + \rho_c)A_c/EI]^{1/2},\ z^* = z/D \end{aligned} \tag{1}$$

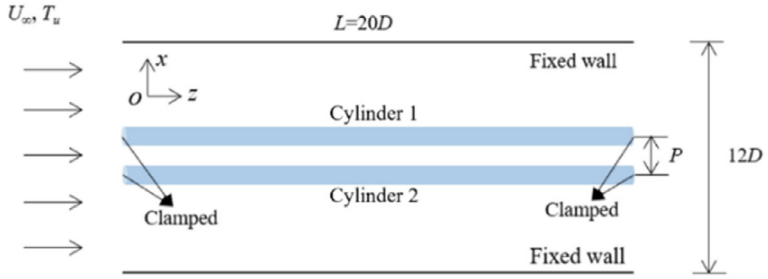


**Fig. 1** Schematic of the two-cylinder system and computational domain

where $C_p$, $u^*$, $t^*$, $A_x{}^*$, $A_y{}^*$, $f^*$ and $z^*$ are the pressure coefficient, dimensionless flow velocity, time, $x$-displacement, $y$-displacement, vibration frequency and axial coordinate of the cylinders, respectively; $p$, $p_\infty$, $U_\infty$, $\rho$, $L$, $A_c$ and $EI$ are the pressure, free-stream pressure and velocity, fluid density, length, cross-sectional area and flexural rigidity of the cylinder, respectively.

## 3 Results and Discussions

### *3.1 Effect of Space Ratio*

Figure 2 displays the rms of $x$ and $y$-displacements for one of the two parallel cylinders under various $P/D$. As $P/D$ reduces from 1.36 to 1.21, the cylinder $y$-displacement has only a slight variation, however the $x$-displacement jumps to about twice of that at $P/D = 1.57$. It is speculated that the shear layers between the two cylinders becomes more unstable at a sufficiently small gap ratio as hydrodynamical interaction between the two cylinders can take effect, hence leading to a large increase in the $x$-displacement whilst causing no obvious variation in the $y$-displacement due to the absence of neighbouring cylinders laterally.

### *3.2 Effect of Inflow Velocity*

Figure 3 shows the transient variations of dimensionless $x$-displacement of cylinder mid-points at $T_u = 0.7\%$ and different $u^*$. It has been found that both vibration amplitudes of the two elastic cylinders gradually increase as $u^*$ increases, and both cylinders tend to bend outwards and show synchronized vibration patterns. As $u^*$ reaches the critical point, both cylinders start to buckle in the opposite directions. Also, with the increase of $u^*$, the dominant vibration mode converts from second to first mode, whilst the frequency of the first vibration mode gradually decreases.

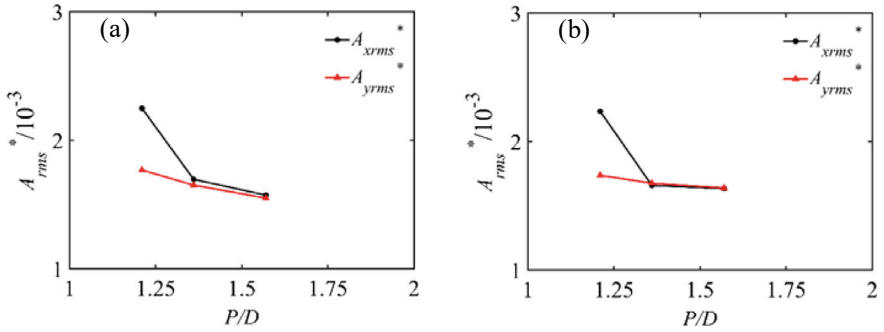


**Fig. 2** The rms of $x$ and $y$-displacements at $u^* = 3.49$ (**a**), 4.56 (**b**) and various $P/D$

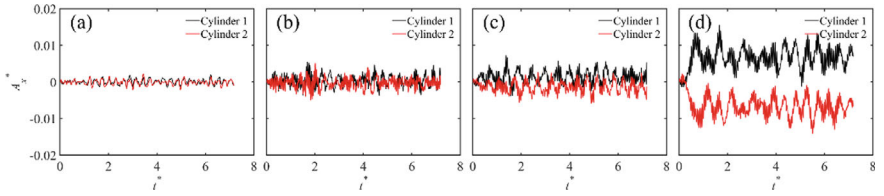


**Fig. 3** $A_x{}^*$ of two cylinders at mid-point and $u^* = 2.04$ (**a**), 3.49 (**b**), 4.56 (**c**) and 5.59 (**d**)

Figure 4 presents the contour of the instantaneous pressure coefficient $C_p$ (a) and instantaneous velocity $U^*$ (b) at $u^* = 5.59$ and $t^* = 5.39$. Figure 4a shows that the pressure distribution is not strictly symmetrical and high-pressure region is evident between two cylinders, causing them to depart away from each other. From Fig. 4b, there exists higher instantaneous velocity of the flow around the two elastic cylinders, implying that the increase of the amplitude aggravates the flow field disturbance. It is speculated from above results that the vibration of the cylinder is mainly affected by the mid to large-scale turbulence in the incident flow. As $u^*$ increases, more turbulent energy accumulates on mid and large-scale eddies, so more intensified vibrations are caused compared with small $u^*$.

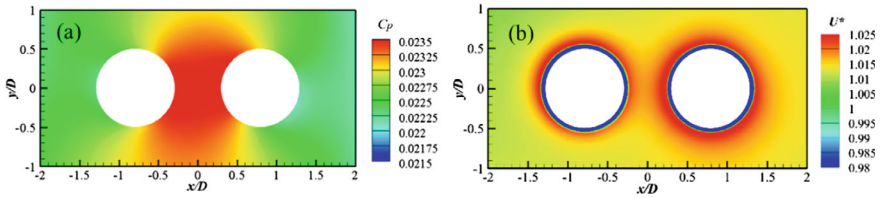


**Fig. 4** Contour of $C_p$ (**a**), and $U^*$ (**b**) in the mid-span cross-section ($u^* = 5.59$, $t^* = 5.39$)

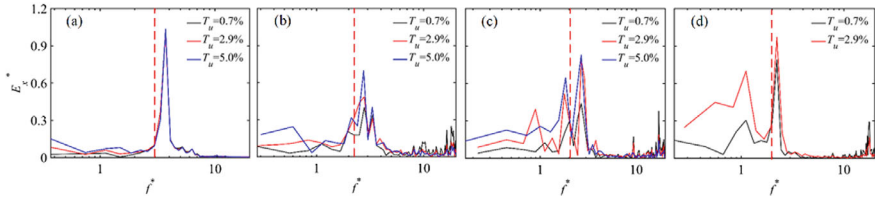


**Fig. 5** Power spectrum density of $A_x{}^*$ at $u^* = 1.20$ (**a**), 3.49 (**b**), 4.56 (**c**) and 5.59 (**d**)

## 3.3 Turbulence Effect

Figure 5 shows the power spectrum density of $A_x{}^*$ at $z^* = 10$ (mid-point) and different $T_u$. It is seen that $T_u$ has no effect on vibration frequency under subcritical condition. However, the transient displacements vary significantly and the two cylinders tend to recover from the outward bending positions as $T_u$ increases. At $u^* = 1.20$, the dominant vibration frequency is close to the natural frequency of the cylinder ($f^* = 3.536$). The vibration is mainly in the first mode, and the second vibration mode is nearly negligible. As $u^*$ increases, there are more peaks appearing near the dominant frequency, which is possibly due to the more complex interactions between the cylinder walls and the large-scale turbulence around the cylinders.

## 3.4 Buckling Instability

Figure 6 presents the time history of dimensionless vibration amplitudes ($A_x{}^*$ and $A_y{}^*$) of two cylinders during buckling conditions. The buckling instability arises at $u^* = 6.0$. It is seen that the $A_x{}^*$ of two cylinders increases continuously and then almost stabilises at 0.06, but the $A_y{}^*$ is nearly negligible. As $u^*$ increases to 6.2, the dimensionless $x$-displacement enhances further to about 0.2, and the $y$-displacement is still close to zero when stabilised. Above results indicate that the hydrodynamic coupling between cylinders and fluid is much more pronounced in the $x$ direction than the $y$ direction.

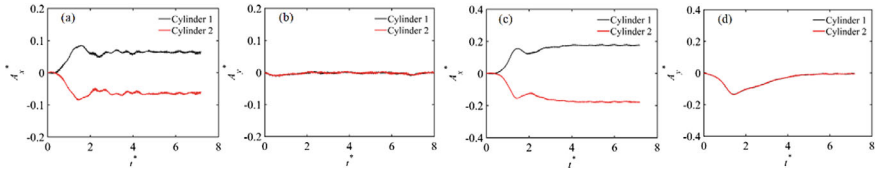


**Fig. 6** Time history of $A_x{}^*$ of two cylinders in $x$ (**a**, **c**) and $y$ (**b**, **d**) direction at $u^* = 6.0$ (**a**, **b**) and 6.2 (**c**, **d**), $z^* = 10$

## 4 Conclusions

LES simulations are carried out to study the AFIV characteristics of two parallel elastic cylinders. A strong coupling effect between the two cylinders have been observed: (1) for small gap ratio, the vibration amplitude is more pronounced in the $x$ direction than $y$ direction, which may be caused by the unstable shear layers between two cylinders; (2) the vibration amplitude of two cylinders increases gradually as $u^*$ increases, and both cylinders tend to bend outward and show synchronized vibration patterns; (3) there is a stable high-pressure region between two cylinders, and the random fluctuations of the above pressure field resulted in considerable subcritical vibrations; (4) $T_u$ does not change the vibration frequency at all flow velocities examined though would cause a significant increase of the vibration amplitude.

**Acknowledgements** This work was supported by CGN-HIT Advanced Nuclear and New Energy Research Institute (Grant No. CGN-HIT202208).

## References

1. Paidoussis MP (1987) Flow-induced instabilities of cylindrical structures. Appl Mech Rev 40(2):163–175
2. Wang L, Ni Q (2009) Vibration of slender structures subjected to axial flow or axially towed in quiescent fluid. Adv Acoust Vib 2009:1–19
3. De Ridder J, Doaré O, Degroote J, Van Tichelen K, Schuurmans P, Vierendeels J (2015) Simulating the fluid forces and fluid-elastic instabilities of a clamped–clamped cylinder in turbulent axial flow. J Fluids Struct 55:139–154
4. Ridder JD, Tichelen KV, Degroote J, Vierendeels J (2016) Fluid-structure interaction in a cluster of cylinders exposed to axial flow: from low-order models to fully coupled CFD-CSM methods
5. Dolfen H, Van Hauwermeiren D, Bral A, Degroote J (2022) Fluid-structure interaction simulation of a wire-wrapped tube array using overset grids
6. Lu ZY, Wong CW, Zhou Y. Turbulence intensity effect on the axial-flow-induced vibration of an elastic cylinder. J Fluids Struct 99